CHANG CHEN
SHIQIANG SONG
JIKUN GUO
QIXIN ZHANG
SHIFU ZHANG
and
TINGAO SHEN

CFD analysis on internal flow field of liquid level control valve under steady working state

At present, all kinds of liquid level control system is widely used in ground and underground storage tanks and other containers, which plays an important role to ensure the safety of production. Thus, it become an indispensable device of modern oil production and storage. In this paper, the governing equations of the internal flow field of the automatic control valve are established by using the basic theory of computational dynamic fluid and the RNG two equations turbulence model. And, the internal flow field of the automatic control valve under steady working state is simulated by using Fluent CFD software. Then, the pressure diagram, velocity profiles figure, velocity vector diagrams were obtained. It is believed that the research results of this paper have reference value for the further optimization of liquid level control valve.

Keywords: *Numerical research, internal flow field, liquid level control valve, steady working state.*

1. Introduction

Oil level control generally refers to the control of the liquid level of the storage tank to keep it at a certain height to avoid oil spills and other safety incidents. At present, all kinds of liquid level control system is widely used in ground and underground storage tanks and other containers, which plays an important role to ensure the safety of production. Thus, it is an indispensable device of modern oil production and storage. Liquid level automatic control valve has the advantages of small volume, simple structure, reliable performance, easy installation and so on, and has been widely used in engineering field.

There was considerable amount of literature on this important area. Eatwell, W. D analyzed the importance and economy of installation of liquid level control value in normal maintenance and well formation protection (Eatwell, 1988). Edwards H W proposed a liquid level control apparatus for a flush tank which includes an upstanding fill tube integral at its upper end with a valve housing carrying a flexible resilient pinch tube valve member and a pivoting actuator engageable with the pinch tube for opening and closing the valve (W, 1999). Khoei, A presented a fuzzy-based controller chip to control the level of a tank (Khoei, et al., 2005). Wang, Zhan Yong designed the test system for refuelling control valve and liquid level controller (Wang, et al., 2008). According to the real structure and work condition of a large-scale gas control valve used in recycling generating electricity project, Cao, Fang set up a fluid-structure interaction system model of control valve, and studied the coupling of fluid and valve plug (Cao, et al., 2011). Zhang, Zhongzhen emphatically analyzed the causes for the failure of level control valve in absorber to the ammonia purification unit and improved the valve internal structure aiming at the failure causes (Zhang, et al., 2011). Buchtel, Michael E present the fluid level control value device and illustrated its using method in detail (Buchtel, 2012). Liu, Changfeng provided information about a new liquid level sensor with TDR technology and a robust motor valve which will work together to make the refrigeration system operating in a safe and energy-saving way with easier service (Liu, 2013). Qian, Jin Yuan established the mathematical model of PCGV and employed computational fluid dynamics (CFD) method is to numerically simulate its dynamic characteristics. Through the analysis of the internal flow field distribution, its working principle is verified. Then three different opening processes with the same spring stiffness are analyzed under different static inlet pressures, and the best design point is obtained by studying the characteristic curves of the valve core's displacement (Qian, et al., 2014). Wang, Yaping conducted the numerical simulation of internal flow field of level control value of water storage tank for the purpose of optimizing the value structure (Wang, et al., 2014). Farooq F R described the design of a simple fuzzy logic liquid level controller. On entering the required liquid quantity with the help of keypad, fuzzy logic controller adjusts the valve

Messrs. Chang Chen, Jikun Guo, Professor, Service Command Department, Qixin Zhang, Associate Professor, Oil Department, Shifu Zhang, Professor, National Engineering Research Center for Disaster & Emergency Relief Equipment and Tingao Shen, Lecturer, Oil Department, Army Logistics University of PLA, Chongqing 401 331 and Shiqiang Song, Master Degree, Logistics Training Center of PLA Rocket Force, Hebei 075 000, China. Corresponding author Mr. Chang Chen, e-mail: 408430734@qq.com

opening and closing in order to supply the desired liquid amount. The performance of the controller is also compared to the proportional control and it is found that fuzzy logic controller is better choice owing to its smoothness and accuracy (R, et.al., 2016). Sumit Kumar designed and comparatively analyzed the P, PI, PID and fuzzy logic controller for coupled tank liquid level system, and set up the simulink model for coupled tank system within MATLAB/ Simulink (S and P, 2017).

However, we have noticed that the literature about the numerical simulation of internal flow field of liquid control value under steady working state is limited. And we demonstrate through an extensive literature review that the existing models are not capable of handling the specifics of problem in this study.

Different from previous studies, this paper established the governing equations of the internal flow field of the automatic control valve by using the basic theory of computational dynamic fluid and the RNG *k*-*ε* two equations turbulence model. The finite volume method has been used to discretize the equations. The internal flow field of the automatic control valve under steady working state is simulated by using Fluent CFD software.

2. Basic theory and algorithm

2.1 Turbulence model

Several turbulence models widely used in engineering include zero-equation model, single-equation model, two-equation model and Reynolds stress model (Wu and Han, 1988). Various models have their adaptability and limitations. Compared to other models, the application of the two-equation model is extensive. What is more, the RNG *k*-*ε* model is further modified according to the difference of the standard *k*-*ε* model in the flow field analysis. The modified *k*-*ε* model is easy to be corrected and the simulation result is better, and more practical (Chen, et al., 2003, (Gao, et al., 2002, (Wang and Wu, 2004, (Yuan, et al., 2006). Therefore, the RNG *k*-*ε* two-equation model is used to simulate the internal flow field of the liquid level control valve. The RNG *k*-*ε* (renormalization, group) model was first proposed by Yakho and Orzag (Yakhot and Orszag, 1986). The basic transport equation is presented as follow (V. Patankar and Zhang, 1984).

Transport equation of turbulent kinetic energy *k*:

$$\frac{\partial k}{\partial t}+\overline{u}_j\frac{\partial k}{\partial x_j}=\frac{\partial}{\partial x_j}\left[\left(\upsilon+\frac{\upsilon_T}{\sigma_k}\right)\frac{\partial k}{\partial x_j}\right]+P_k-\varepsilon \quad \text{...} \quad (1)$$

Transport equation of turbulent energy dissipation ε :

$$\frac{\partial \varepsilon}{\partial t}+\overline{u}_j\frac{\partial \varepsilon}{\partial x_j}=\frac{\partial}{\partial x_j}\left[\left(\upsilon+\frac{\upsilon_T}{\sigma_\varepsilon}\right)\frac{\partial \varepsilon}{\partial x_i}\right]+C_1\frac{\varepsilon}{k}P_k-C_2\frac{\varepsilon^2}{k}-R \quad \text{...} \quad (2)$$

$$P_k=\upsilon_T S^2=2\upsilon_T\overline{S}_{ij}\overline{S}_{ij} \quad \text{...} \quad (3)$$

$$\overline{S}_{ij}=\frac{1}{2}\left(\frac{\partial \overline{u}_i}{\partial x_j}+\frac{\partial \overline{u}_j}{\partial x_i}\right) \quad \text{...} \quad (4)$$

$$R=\frac{C_u\eta^{-3}\left(1-\overline{\eta}/\eta\right)}{1+\beta\eta^{-3}}\frac{\varepsilon^2}{k} \quad \text{...} \quad (5)$$

$$\overline{\eta}=\left(\overline{S}_{ij}\overline{S}_{ij}\right)^{1/2}k/\varepsilon \quad \text{...} \quad (6)$$

In the above formula, P_k represents turbulent kinetic energy produced by the mean velocity gradient (unit: *J*). *S* represents the average coefficient of strain tensor. $\overline{S}_{ij}$ represents the mean strain force (unit: *N*). *R* represents the additional dissipation generating term, representing the effect of average strain rate on *ε*. $\overline{\eta}$ represents the ratio of turbulent time to strain scale, and it normally $\eta_0 = 4.38$, $\beta = 0.015$. Other constant coefficients of RNG *k*-*ε* model are listed in Table 1.

Table 1: Constant coefficient of RNG κ–ε model

C_μ	σ_k	σ_ε	C_1	C_2
0.085	0.7179	0.7179	1.42	1.68

2.2 Discretization of turbulence equations

To solve the governing equations by numerical method, the governing equations must be discretized. With the development of computational fluid dynamics, the main discretization methods include finite difference method, finite element method and finite volume method and so on. Among them, the finite volume method is widely used in the field of CFD in recent years, which is characterized by high computational efficiency. This method is adopted in fluent software. Finite volume method (FVM) (Wang, 2004), also known as control volume method (CVM), which is proposed by Jameson et al. In principle, the finite volume method can deal with any geometric shape and curve mesh flow problem (Li and E, 1994). The basic idea is to divide the calculation area into a limited number of non-overlapping meshes, each of which is a control volume. And the center of the control volume is taken as the computational node. The differential equation (control equation) is integrated in the control volume to obtain a set of discrete algebraic equations with the dependent variable of the control volume calculation node. The finite volume method is to calculate the discrete value by using the interpolation function to calculate the control volume without considering the change of the dependent variable between the compute nodes. The discrete functions used in the process of discretization of control equations are also called discrete formats. The commonly used discrete formats are: central difference scheme, upwind differential format, mixed format, power function format, and QUICK format.

2.3 SIMPLE algorithm

The SIMPLE algorithm is a numerical method mainly used to solve the incompressible flow field calculation problem, which is proposed by Patanker, Spalding et al. in 1972 (Liu, 2007). SIMPLE algorithm is the abbreviation of semi-implicit method for pressure-linked and equation, which is a semi-implicit method for solving the pressure-coupled equations. The SIMPLE algorithm is roughly divided into two steps: the estimated step and the calibration step. The estimated step is to solve the velocity field by using the discrete momentum equation according to the given pressure field. Since the given pressure field in the estimation step is the assumed value or the previous iteration value, so the speed field obtained in this way is generally unable to meet the continuity equation, then it is essential to enter the next calibration step. The corrected pressure field is substituted into the next level of iteration for calculation, so repeatedly, until the convergence of the solution is obtained.

(1) Discretization of momentum equations:

$$a_p u_p = \sum_{E=1}^{N_s} a_E u_E - \sum_{e=1}^{N_s} p_e (\Delta y)_e + b_p \quad \dots \quad (7)$$

$$a_p v_p = \sum_{E=1}^{N_s} a_E v_E - \sum_{e=1}^{N_s} p_e (\Delta x)_e + b_p \quad \dots \quad (8)$$

In equations (7) and (8), e represents each interface of the control volume P. P_e represents the pressure on the interface e. $(\Delta x)_e$ represents the deference of x coordinate value between the end point and the start point of the interface e. $(\Delta y)_e$ represents the deference of y coordinate value between the end point and the start point of the interface e. The velocity equation of the control volume interface is:

$$\begin{cases} u_e = \left(\dfrac{\sum_{E=1}^{N_S} a_E u_E + b_p}{a_p} \right) - \left(\dfrac{\Delta y}{a_p} \right)_e (p_E - p_P) \\ v_e = \left(\dfrac{\sum_{E=1}^{N_S} a_E v_E + b_p}{a_p} \right) - \left(\dfrac{\Delta x}{a_p} \right)_e (p_E - p_P) \end{cases} \quad \dots \quad (9)$$

(2) Establishment of velocity correction equation:

The velocity correction equation at the control volume interface is:

$$u'_e = \left(\frac{\Delta y}{a_p} \right)_e (p'_P - p'_E) \quad \dots \quad (10)$$

$$v'_e = \left(\frac{\Delta x}{a_p} \right)_e (p'_P - p'_E) \quad \dots \quad (11)$$

The velocity correction equation at the control volume node is:

$$u'_p = \sum_{e=1}^{N_S} \left[-p'_e \left(\frac{\Delta y}{a_p} \right)_e \right] \quad \dots \quad (12)$$

$$v'_p = \sum_{e=1}^{N_S} \left[-p'_e \left(\frac{\Delta x}{a_p} \right)_e \right] \quad \dots \quad (13)$$

The values α_p in equations (12) and (13) represent the values in equations (7) and (8) respectively. The pressure p_e on each interface of the control volume can be obtained based on the linear interpolation method by calculating the pressure correction value at the calculated node within the adjacent control volume P and E. For the specific pressure field p^*, the corresponding velocity u_p and v_p can be solved by the momentum discrete equations (7) and (8), and the two speeds are denoted as u^*_p and v^*_p respectively. Combined with the velocity correction equations (12) and (13) on the calculation node, the correction speed on the control volume calculation node can be obtained as follow:

$$U_p = u^*_p + u'_p \quad \dots \quad (14)$$

$$V_p = v^*_p + v'_p \quad \dots \quad (15)$$

The velocity u^*_e and v^*_e at the control volume interface are calculated by substituting the velocity u^*_p and v^*_p into the equations (9). Then, the correction speed on the control volume interface is obtained by combined with the velocity correction equations (10) and (11) on the interface:

$$u_e = u^*_e + u'_e = u^*_e + \left(\frac{\Delta y}{a_p} \right)_e (p'_P - p'_E) \quad \dots \quad (16)$$

$$v_e = v^*_e + v'_e = v^*_e + \left(\frac{\Delta x}{a_p} \right)_e (p'_P - p'_E) \quad \dots \quad (17)$$

(3) Establishment of pressure correction equation

Pressure correction equation:

$$a_p p_p = \sum_{E}^{N_S} a_E p_E + b_p \quad \dots \quad (18)$$

Equation coefficient:

$$a_E = \left[\left(\frac{\rho \Delta y^2}{a^u} + \frac{\rho \Delta x^2}{a^v} \right)_e \right]_E \quad \dots \quad (19)$$

$$a_p = \sum_{E}^{N_S} a_E \quad \dots \quad (20)$$

$$b_p = \sum_{E}^{N_S} \left[(\rho u^* \Delta y)_e - (\rho v^* \Delta x)_e \right]_E \quad \dots \quad (21)$$

In the above formula, α^u represents the parameter α_p in the momentum equation u (7), and α^v represents the parameter α_p in the momentum equation (8). The pressure correction value p_p on the calculation node can be solved according to equation (18), and the pressure correction value p_ε on the control volume interface is obtained by linear interpolation. The corrected pressure field is calculated according to equation (22):

$$P_p = p^*_p + p'_p \quad \dots \quad (22)$$

(4) SIMPLE algorithm calculation steps

The SIMPLE algorithm on the unstructured grid is calculated as follows:

Step 1, given a pressure field initial value p^* ;

Step 2, calculate the speed u^* and v^* corresponding to the pressure field p^* from equation (7) and (8);

Step 3, calculate the interface speed u^*_e and v^*_e from equation (9);

Step 4, calculate the coefficients and source terms of the pressure correction equation from equation (19), (20) and (21);

Step 5, calculate the pressure correction value p'_p on the control body calculation node from equation (18);

Step 6, calculate the velocity correction value u'_p and v'_p on the control body calculation node from equation (12) and (13);

Step 7, calculate the corrected speed u, v and pressure p from equation (14), (15) and (22);

Step 8, the judgment of the convergence of the results. If it does not converge, go back to step 2 and start the calculation until the result is converged.

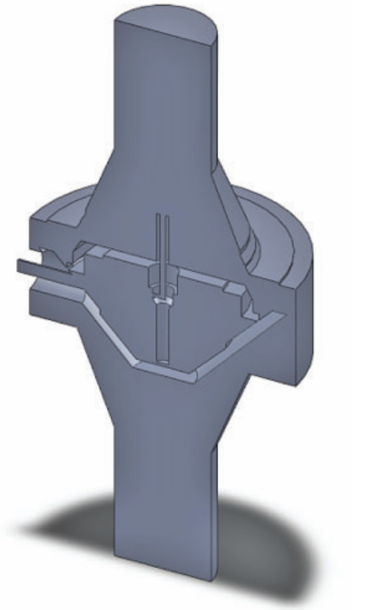

Fig.1 Geometric model of control valve internal flow field (cross-section drawn)

Fig.2 Mesh grids of calculation model

3. Establishment of geometric model

The numerical simulation of the internal flow field of the liquid level control valve requires the establishment of appropriate geometric models and mathematical models. The rationality of the mathematical model has a decisive effect on the numerical simulation results. The establishment of the model must follow two principles: one is the physical authenticity of the model; the second is the feasibility of mathematical calculation. The physical authenticity requires that the geometric model established reflect the characteristic of the computational object as much as possible so as to guide the practical application. The feasibility of mathematical calculation is that the model must be simplified to the extent that the current mathematical tools can solve. According to the above principles and the basic structure and size of the control valve, a geometric model of the internal flow field of the level control valve in full open state is established by using the SolidWorks software. The cross-section drawn of the geometric model are shown in Fig.1. In the process of establishing the geometrical model, considering the complexity of fluid flow at the inlet and outlet of the liquid control value, a 100 mm long pipe is set up at the inlet and outlet positions of the control valve. Simultaneously, as in the simulation process, the main concern is the velocity and pressure distribution of internal flow field, so some unnecessary structures of the value have been simplified.

4. Mesh generation

In the process of numerical simulation, the calculation area should be meshed first. The rationality of grid division directly determines the accuracy and convergence of numerical calculation. In this paper, the geometric model established by the SolidWorks software is introduced into the Gambit software for grid generation which is shown in Fig.2. Because the computational model is complex, the tetrahedron unstructured grid is used for meshing, and the mesh is properly encrypted for the special position near the throttle.

5. Determination of boundary conditions

The calculation of the flow field is generally relative to a certain boundary condition. The setting of the boundary condition requires the adaptability in mathematics, rationality in physics, and also considers the convergence and precision of the calculation. According to the actual flow characteristics and passageway characteristics inside the level control valve, the following boundary conditions have been selected.

Import: set pressure inlet (pressure inlet) boundary conditions.

Export: set pressure outlet (pressure outlet) boundary conditions.

Wall: all boundaries except the entrance and exit are set as fixed wall conditions.

6. Solver and parameter setting

Start FLUENT 3D single-precision version, and select pressure-based steady-state implicit solver. Turbulent model select the RNG two equation model. Fluid material is set to water, and its density is modified to 1000 kg/m^3. Operating conditions remain the default settings, and the entire process ignores gravity effects. The inlet pressure is set to 3750 Pa. The turbulence is defined as the intensity and hydraulic diameter, and the turbulence intensity is set 5%, the hydraulic radius is set to 80 mm, and the outlet pressure is set to 0 Pa.

The convergence factor of the solver is set as: pressure equal 0.3, density equal 1, volume force equal 1, momentum equal 0.7, turbulent kinetic energy equal 0.8, turbulent dissipation rate equal 0.8, and turbulent viscosity equal 1. SIMPLE algorithm is chosen as pressure-speed coupling algorithm. All residual convergence accuracy is defined as 0.0001. In order to monitor the change of those parameters, mass flow monitors have been set up at the inlet and outlet of the control value respectively.

7. Results and analysis

The iterative calculation begins when the flow field is initialized. When the number of iterations reaches 570 times, the result is converged and the iterative calculation ends. The residue monitoring curves and the mass flow monitoring chart are shown in Fig.3 and Fig.4. It can be seen from the residual graph that the continuity curves of the continuity, ε, *k* and x, y, and z directions converge well. Import and export mass flow tends to be stable. Import mass flow was 6.6505504 kg/s, and export mass flow was 6.6505594 kg/s. According to the law of conservation of mass, it can see that the calculation result is correct.

After the iteration calculation, the velocity and pressure distributions of the flow field can be obtained, which provide a reliable basis for describing the internal basic flow regime of the liquid level control device. In order to detailed analyze the pressure and velocity distribution in internal flow field and at the orifice position, a Z = 0 cross section is established, through which the pressure and velocity distribution of the flow field and the orifice can be clearly observed. Figs.5 to 11 show the pressure distribution, velocity distribution, velocity vector distribution and streamline diagram (pressure unit Pa, velocity unit m/s) for the flow field outer surface and Z = 0 cross section.

From the above calculation results, it can be seen that the inlet mass flow rate of the automatic control valve and the float valve calculated by the Fluent CFD software is stable at 6.6505504 kg/s and the outlet mass flow rate is stable at 6.6505594 kg/s. The mass flow error is 0.135×10^{3}%< 0.5%, which meeting the quality of conservation. It can be seen from the pressure distribution diagrams (Figs.5 and 6) that the pressure distribution of inlet and outlet are relatively uniform, which was 2.98×10^{3} Pa and -1.18×10^{-2} Pa. The maximum pressure appears in the upper chamber of the value core which is approximately 3.77×10^{3} Pa. Basically the same is

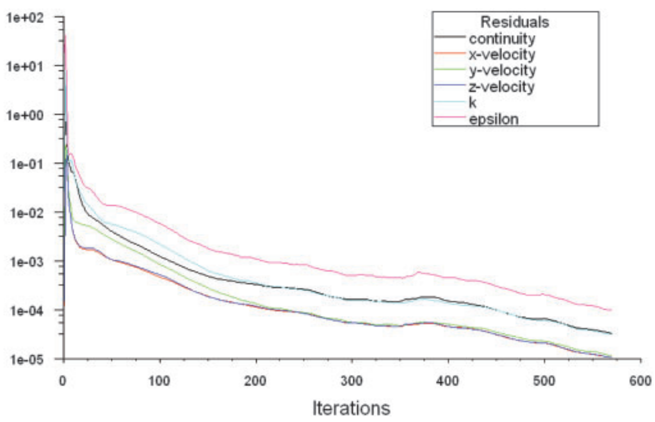

Fig.3 Residue monitoring curves

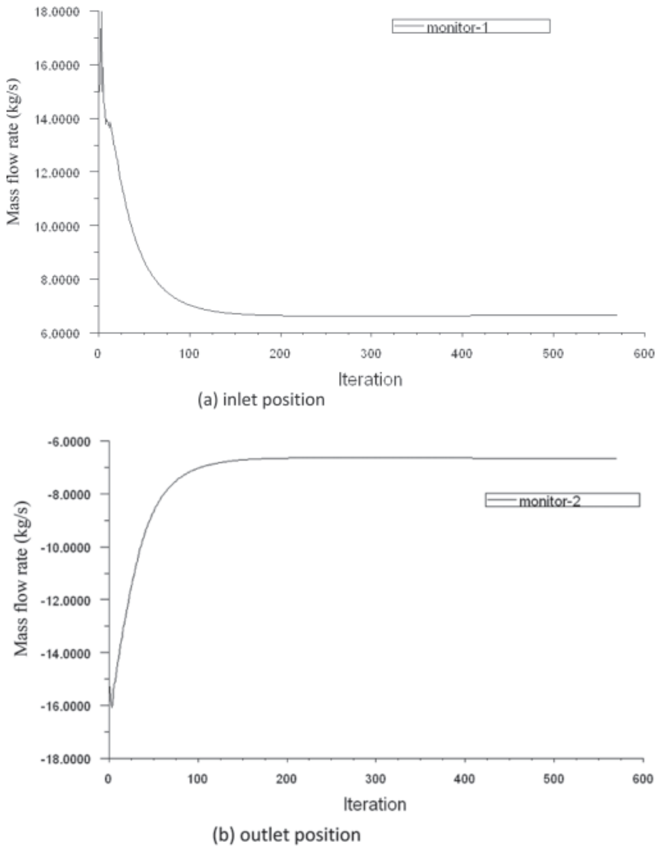

Fig.4 Quality flux curve of inlet and outlet

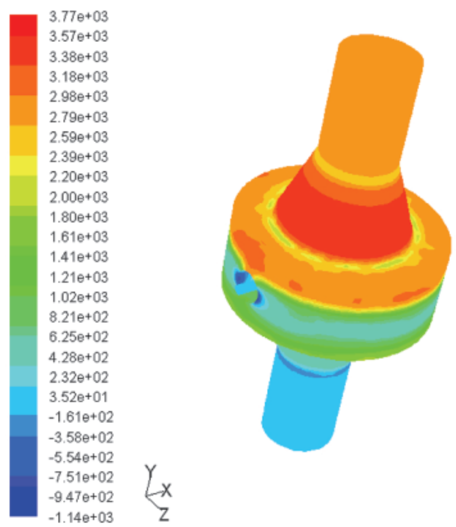

Fig.5 Pressure contours of exterior surface

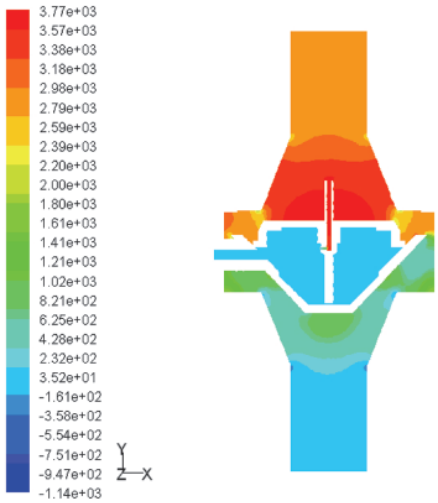

Fig.6 Pressure contours of Z = 0 plane

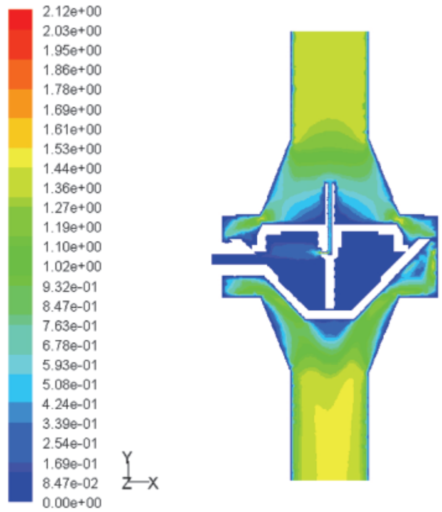

Fig.7 Velocity contours of Z = 0 plane

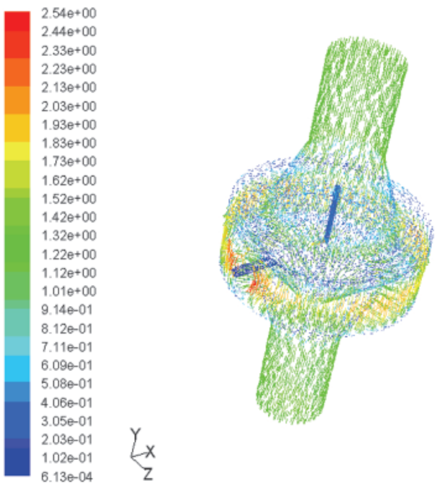

Fig.8 Velocity vectors of exterior surface

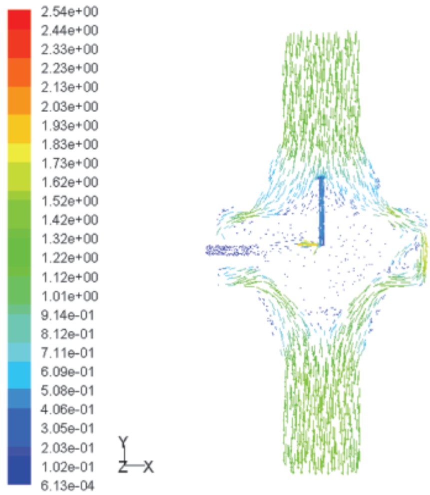

Fig.9 Velocity vectors of Z = 0 plane

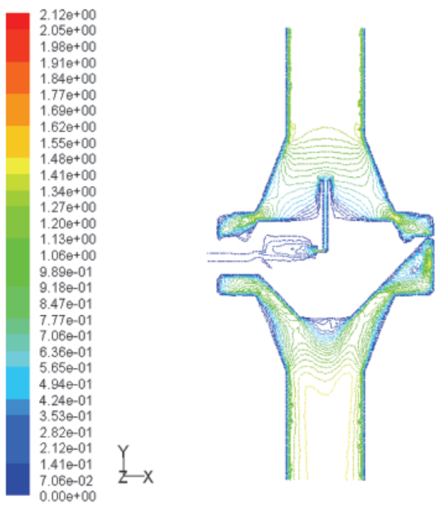

Fig.10 Velocity isoclines of Z = 0 plane

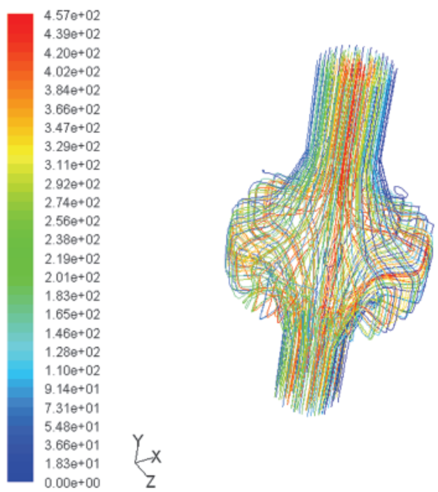

Fig.11 Streamline diagram

with the opening pressure of the automatic control valve, the pressure inside the chamber of the value core is about 0 Pa. The pressure difference between the upper chamber and the internal chamber of the value core ensures the opening and stabilizing operation of the liquid level control valve.

From the velocity distribution diagrams (Fig.7), the liquid flow inside the automatic control valve is relatively stable. There is no vortex and other unstable flow, which guarantees the work stability of the value. The flow rate of the liquid inside the automatic control valve is slower than that of the inlet and outlet position, which is due to the increase in the cross-section area of the inside of the valve. The liquid enters the internal chamber of the value core through the orifice and reaches its maximum flow rate approximately 2.12 m/s. The larger flow rate of liquid may lead to a certain imbalance force. From the velocity vector diagram (Figs.8 and 9), the velocity contour (Fig.10), and streamline diagram (Fig.11) it can be seen that the flow of the fluid is relatively uniform. Since the wall viscosity is large, the velocity of the fluid near the wall is close to zero, indicating that the simulation of the RNG model and the wall function method is reasonable.

8. Conclusion

In this paper, the governing equations of the internal flow field of the automatic control valve are established by using the basic theory of computational dynamic fluid and the RNG two equations turbulence model. The finite volume method is used to discretize the equations. The internal flow field of the automatic control valve under steady working state is simulated by using Fluent CFD software. And the pressure diagram, velocity profiles diagram, velocity vector diagrams and streamlines diagram were obtained. The numerical simulation results show that the fluid at the inlet and outlet of the control value is basically a developed flow when the automatic control valve maintain stable operation. At the wall, the velocity of the control valve is almost zero due to the influence of the viscous force. There is no imbalance force in the control valve. What is more, due to the effect of the orifice, there is a large pressure difference between the upper and internal chamber of the value core, so that the valve can open and maintain a stable operation. These conclusions provide a theoretical basis for the technical design and improvement of the control valve.

Acknowledgments

This paper is supported in part by The National Key Technology R&D Program of China (2017YFC0806306), Education Science fund of the Military Science Institute of Beijing, China (No.2016JY481), and Chongqing Graduate Scientific Research Innovation Project, China (No.CYB17148).

Conflicts of interest

The authors declare that there are no conflicts of interest regarding the publication of this paper.

References

1. Buchtel, M. E. (2012): Fluid level control toggle valve device and method: US, 8,091,581 [P]. 2012-1-10.
2. Cao, F., Wang, Y., Yantao, A. N. and Xie, Y. (2011): "Fluid-structure Interaction Analysis for Large-scale Gas Control Valve." *Machine Tool & Hydraulics*, 455(11): 146-150.
3. Chen, Q., Xu, Z. and Zhang, Y. (2003): "Application of RNG k-ε Models in Numerical Simulations of Engineering Turbulent Flows." *Chinese Quarterly of Mechanics*, 24(1): 88-95.
4. Eatwell, W. D. (1988): Liquid level control subsurface valve reduces workover expense in artificial lift pump installations; proceedings of the SPE Annual Technical Conference & Exhibition, October 2, 1988 - October 5, 1988, Houston, TX, USA, F, 1988 [C]. Publ by Soc of Petroleum Engineers of AIME.
5. Gao, H., Fu, X., Yang, H. and Tsukiji, T. (2002): "Numerical and Experimental Investigation of Cavitating Flow within Hydraulic Poppet Valve." *Chinese Journal of Mechanical Engineering*, 38(8): 27-30.
6. Khoei, A., Hadidi, K., Khorasani, M. R. and Amirkhanzadeh, R. (2005): "Fuzzy level control of a tank with optimum valve movement." *Fuzzy Sets and Systems*, 150(3): 507-523.
7. Li, F. and E, Q. (1994): "Analysing and Improving of the Finite Volume Scheme." *Acta Aerodynamica Sinica*, 12(4): 465-470.
8. Liu, C. (2013): "Application of new type liquid level sensor and motor valve into liquid level control." *Refrigeration and Air-Conditioning*, 13(3): 26-29.
9. Liu, M. (2007): Computational fluid and heat transfer mass transfer [M]. Hefei:Press of University of Science and Technology of China, 2007.
10. Qian, J. Y., Wei, L., Jin, Z. J., Wang, J. K., Zhang, H. and Lu, A. L. (2014): "CFD analysis on the dynamic flow characteristics of the pilot-control globe valve." *Energy Conversion & Management*, 87220-226.
11. R, F. F., G., A. and U, A. (2016): "A Simplified Fuzzy Logic Liquid Level Control System." *Journal of Intelligent Computing*, 7(4): 135-144.
12. S, K. and P, N. M. (2017): "Comparative Analysis of P, PI, PID and Fuzzy Logic Controller for tank water level control system." *International Research Journal of Engineering and Technology*, 4(4): 1174-1177.
13. V. Patankar, S. and Zhang, Z. (1984): Numerical calculation of heat transfer and fluid flow [M]. Beijing: China Science Publishing & Media Ltd., 1984.
14. W, E. H. (1999): Pinch tube tank level control valve with snap-action shutoff: U.S, 5, 896, 887 [P]. 1999-4-27.
15. Wang, F. (2004): Computational fluid dynamics analysis – principles and applications of CFD software [M]. BeiJing Tsinghua University Press, 2004.
16. Wang, Y., Gao, L., Ge, J., Gao, H. and Zhang, J. (2014): "The numerical simulation analysis of flow field in level control valve of water storage tank." *International Journal of Control and Automation*, 7(10): 45-52.
17. Wang, Y. and Wu, W. (2004): "Numerical Simulation of Flow Around Blunt Bodies using RNG k-ε Turbulence model." *Journal of University of Shanghai For Science and Technology*, 26(6): 519-523.
18. Wang, Z. Y., Tang, Y. C. and Liu, Z. G. (2008): "The Design of Refuelling Control Valve and Liquid Level Controller Test System." *Chinese Hydraulics & Pneumatics*, 32(7): 16-17.
19. Wu, J. and Han, Q. (1988): The theory, method and application of computational fluid dynamics [M]. Beijing: China Science Publishing & Media Ltd., 1988.
20. Yakhot, V. V. and Orszag, S. A. (1986): "Renormalization-group analysis of turbulence." *Journal of Scientific Computing*, 1(1): 3-51.
21. Yuan, X., He, Z. and Mao, G. (2006): "Nmmerical Simulation of a Turbulence Flow in the Cut-off Value by RNG k-ε Turbulence Model." *Fluid Machinery*, 34(2): 34-38.
22. Zhang, Z., Li, B. and Gao, J. (2011): "Analysis on failure causes for level control value in absorberb and retrofit." *Large Scale Nitrogenous Fertilizer Industry*, 34(1): 31-32.